

Photoluminescence Upconversion in GaAs Quantum Wells

Soheyla Eshlaghi ^a, Wieland Worthoff ^a, A. D. Wieck ^b and Dieter Suter ^a

^aFakultät Physik, Technische Universität Dortmund, 44221 Dortmund, Germany;

^bLehrstuhl für Angewandte Festkörperphysik, Ruhr-Universität Bochum, 44780 Bochum, Germany

ABSTRACT

We present a detailed experimental study of photoluminescence upconversion in GaAs quantum wells over a wide temperature range. The dependence of the upconversion on the well width is discussed and the conversion efficiency is determined as a function of laser detuning. The best results are achieved when the laser detuning is comparable to the thermal energy of the system, $\Delta E \approx 2k_B T$.

Keywords: Laser cooling, luminescence upconversion, GaAs, quantum wells, exciton

1. INTRODUCTION

Since the initial demonstration experiments on laser cooling in solids in 1995 by Epstein and coworkers,¹ there have been extensive efforts to develop this technique. Starting from room temperature, laser cooling by 3 to 80 K has been reported in rare earth doped glasses, using different hosts and dopants.²⁻⁵ In addition to laser cooling of glasses, its application to semiconductor materials was also considered.^{6,7} Advantages of semiconductors compared to rare earth doped materials include the higher absorption coefficient, the potential for much lower temperatures, and the opportunity for direct integration into optoelectronic devices.⁶ The proposed mechanism for laser cooling in semiconductors is phonon-assisted absorption of photons whose energy is below the mean luminescence frequency. The additional energy is provided by phonons. The emitted photoluminescence (PL) is then blue shifted and the difference between the energies of the absorbed and emitted photons is carried out of the lattice by luminescence. This is known as PL-upconversion or anti-Stokes PL (AS-PL), the main prerequisite for laser cooling.

The wide interest in laser cooling of semiconductors and the absence of net laser cooling have motivated extensive theoretical investigations geared toward the determination of the best experimental conditions for cooling.⁸⁻¹⁵ These groups studied the effect of different experimentally accessible parameters on laser cooling, such as the excitation- and carrier density, temperature, and laser detuning, as well as different parasitic processes. One of the models used in this analysis is due to Sheik-Bahae and Epstein,⁸ who considered the conditions for achieving net cooling in undoped bulk GaAs. Their model relies on rate equations for the carrier density. Taking into account the non-radiative recombination rate and the luminescence extraction efficiency, a break-even condition was derived for the non-radiative lifetime. If this condition is exceeded, it should be possible to achieve net cooling. A comprehensive study by Rupper and co-workers¹⁴ is based on a microscopic many-particle theory. They considered the dependence of the net cooling on the carrier density and temperature in undoped bulk GaAs. Several different models were compared, with particular consideration for excitonic effects. It was found that excitonic effects are significant for overcoming the (parasitic) background absorption as well as for a strong reduction of the required non-radiative lifetime, resulting in a dramatic improvement of the cooling criterion. This was attributed to the excitonic enhancement of the low-frequency absorption, which increases the radiative recombination rate. Khurgin discussed the mechanisms which can be responsible for luminescence upconversion in semiconductors and developed a theory of phonon assisted transitions near the direct band gap of semiconductors.¹⁵ In this model, the Urbach tail plays a significant role for the appearance of PL upconversion and therefore for laser cooling applications.

Experimentally observed phonon-assisted AS-PL in semiconductors was first reported by Finkeißen et al.¹⁶ in GaAs/Al_xGa_{1-x}As quantum wells (QWs) for temperatures between 40 and 50 K in magnetic fields and by

email: soheyla.eshlaghi@tu-dortmund.de

Gauck et al. in GaAs/Ga_xIn_{1-x}As heterostructures (GaAs thickness: 0.5-1 μm) at room temperature.¹⁷ In a more recent paper,¹⁸ we presented a detailed study of the anti-Stoke PL as a function of temperature and excitation energy in GaAs/Al_{0.35}Ga_{0.65}As QWs.

In this paper, we discuss the dependency of the PL-upconversion on excitation energy, temperature in GaAs/Al_{0.35}Ga_{0.65} QWs and present the results of anti-stokes PL measurements for different well widths. The sample under study and its PL characteristics is described in Sec.2. In Sec.3 we outline the temperature dependence and discuss the efficiency of the AS-PL as a function of temperature and laser detuning. Further we discuss the conversion between the heavy and light-hole states. Section 4 compares the measurement results of AS-PL for QWs with different widths. The results are summarized in the last section.

2. EXPERIMENTAL

2.1 The sample and experimental conditions

The sample used in our study was grown by molecular beam epitaxy on a Te-doped GaAs substrate and consists of 13 undoped GaAs/Al_{0.35}Ga_{0.65}As QWs whose thickness varies from 2.8 to 39.3 nm. The thickness of the Al_{0.35}Ga_{0.65}As barriers is about 31 nm, therefore there is no coupling between different QWs.

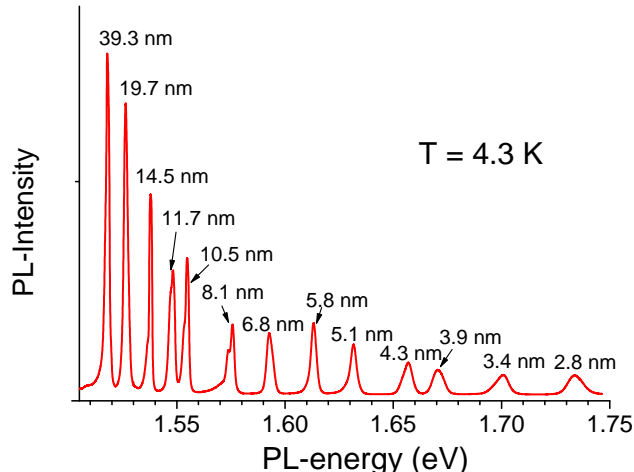


Figure 1. PL-Spectrum of the sample at $T = 4.3$ K. The sample consists of 13 QWs with various thicknesses. The well widths are indicated in the figure.

Fig.1 shows the photoluminescence (PL) spectrum of the sample at $T = 4.3$ K. The excitation source was a laser diode with an energy of 1.94 eV (638 nm). The thickness of the QWs decreases from the substrate toward the surface, so that the PL from the deeper QWs is not absorbed in the upper layers. The amplitude of the different PL lines is roughly proportional to the thickness of the corresponding QW. The line widths increase with decreasing well width due to increasing influence of the interface roughness.

For all measurements presented in the next sections, the excitation source was a cw titanium sapphire laser with a tunable wavelength range between 750-825 nm (1.50-1.65 eV). The sample was mounted on the cold finger of a He flow cryostat. An Oxford ITC 502 temperature controller and heater were used to control the sample temperature. The photoluminescence was collected by two lenses and passed through a 1 m monochromator (SPEX 1794). A thermoelectrically cooled charged coupled device (CCD) (1024×256 , pixel size $27 \mu\text{m}$) was used as detector. The spectral window of about 20 nm allows us to detect the PL of several QWs and the scattered light of the laser simultaneously. The excitation intensity was about 50 W/cm^2 (corresponding to a photo generated carrier density of about $N_c \approx 10^{15} \text{ cm}^{-3}$ assuming an absorption coefficient of $4 \times 10^4 \text{ cm}^{-1}$ and a carrier lifetime of 1 ns^{19-21}).

2.2 PL upconversion

PL upconversion can be detected for most of the QWs from liquid He temperature up to room temperature. Fig. 2a shows some anti-Stokes (solid lines) and Stokes-PL (dashed lines) spectra of the 5.1 nm QW. For this measurements the temperature was kept constant at $T = 54$ K, while the laser wavelength was set to different wavelengths near the emission wavelength of this QW. The narrow lines correspond to the laser, the broader lines, whose position is constant (1.631 eV) corresponds to the exciton resonance. Clearly the PL signal increases when the laser wavelength comes closer to the resonance line, but the signal from the exciton line remains well observable for a laser detuning of a several meV, for the Stokes as well as for the anti-Stokes case.

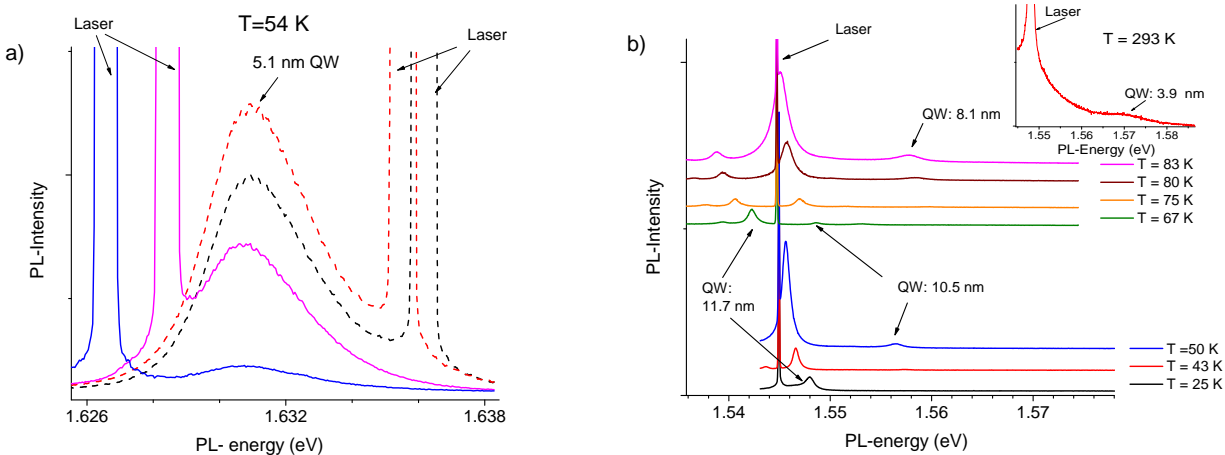


Figure 2. a) PL spectra of the 5.1 nm QW at $T = 54$ K (mean PL energy: 1.631 eV). The dashed lines represent the Stokes, the solid ones the anti-Stokes PL. b) Anti-Stokes PL-spectra at various temperatures. New PL-lines appear on the anti-Stokes side when the thermal energy exceeds the laser detuning ΔE for the corresponding QWs. The inset shows the AS-PL of the 3.9 nm QW at room temperature ($T = 293$ K).

Fig. 2b shows some PL-spectra for the case that the laser energy was kept constant (1.5447 eV) while the temperature was varied between 25 and 83 K. At $T = 25$ K in the AS region, only the PL of the 11.7 nm QW can be observed. With increasing temperature, the band gap decreases and the resonance of this QW moves closer to the laser energy, and its amplitude increases. At temperatures above 60 K, the resonance line of the 11.7 nm QW has moved to the Stokes side of the laser line and its amplitude decreases again. This is clearly the typical behavior expected for the offset dependence of a resonant excitation. The same behavior is observed for the 10.5 nm QW, which first becomes visible at a temperature of 50 K, as the thermal energy of the system becomes comparable to the detuning between the laser energy and the PL-energy of the 10.5 nm QW. It moves into resonance at 84 K. At temperatures above 80 K, the resonance line of the 8.1 nm QW also becomes visible, indicating that the thermal energy is now sufficient for an anti-Stokes shift of about 16 meV.

As the temperature increases further, the PL-lines of the thinner QWs appear, the line positions shift to lower energy, eventually crossing over to the Stokes side of the spectrum. The inset of the fig. 2b) shows the AS-PL of 3.9 nm QW measured at $T = 293$ K indicating that even thin QWs with a small absorption cross section can emit AS-PL even at room temperature.

3. TEMPERATURE DEPENDENCE

The frequency range, over which anti-Stokes PL can be observed, depends strongly on temperature. In this section, we focus our attention on the 11.7 nm QW and show the measurement results for this QW at various temperatures.

3.1 Detuning dependence

Fig. 3 shows the photoluminescence excitation (PLE) spectra for four different temperatures, from 14.5 K to 73 K. For each measurement series, we tuned the laser wavelength and measured the integrated PL intensity as a function of the detuning $\Delta E = E_{\text{laser}} - E_{\text{PL}}$ while the temperature was kept constant. All measured intensities are normalized (divided by the intensity of the 14.5 nm QW) in order to eliminate the effect of laser power fluctuations.

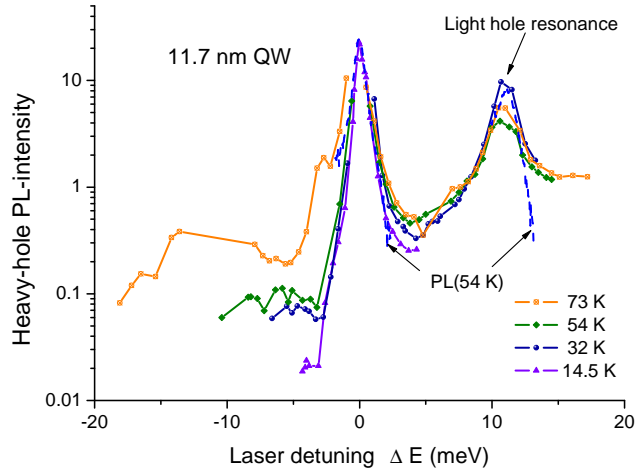


Figure 3. PLE spectra of the hh-PL of the 11.7 nm QW at various temperatures as a function of the laser detuning $\Delta E = E_{\text{laser}} - E_{\text{PL}}$. The blue dashed lines indicate the hh and lh-PL of the QW at 54 K.

The resonant behavior of the absorption process can be seen not only if the laser is resonant with the heavy-hole (hh) transition: when the laser detuning reaches +10.7 meV, we observe an increase in the heavy-hole PL, indicating resonant excitation of the light-hole and a transfer of light-hole to heavy-hole states. The blue dashed lines in the figure indicate the hh and lh-PL of the QW at 54 K. The PL reaches similar values when the laser excites the light-hole transition as for the hh transition, indicating a rather efficient lh to hh conversion.

Fig. 3 also shows how the detuning dependence changes with temperature. On the Stokes-side ($\Delta E > 0$), where the absorption process does not depend on the presence of phonons, the increase of the temperature does not significantly affect the shape of the PLE spectrum. On the anti-Stokes side, however, the increase of the temperature changes the behavior drastically: at $T = 14.5$ K, the anti-Stokes PL decreases rapidly with the laser detuning, becoming unobservable at more than 4 meV, but with increasing temperature, it can be observed even for detunings greater than 15 meV ($T = 73$ K).

The measurements at higher temperatures have a higher detection limit due to presence of LO-phonons. LO-phonons are excited at temperatures above ≈ 50 K and cause significant linewidth broadening at temperatures above 90 K.²²

At $T = 73$ K, in the region between $-13.6 \text{ meV} < \Delta E < -7.9 \text{ meV}$, we have no experimental data. In this region, the laser energy is resonant with the heavy-hole level of the 14.5 nm QW. This results, as we will see also in sec. 3.3, in an increasing of its light-hole PL, which is closed to the heavy-hole transition of the 11.7 nm QW. As a result, and due to line width broadening at the higher temperatures, we cannot reliably measure the PL intensity of the 11.7 nm QW in this range.

For better comparison of the AS-PLE spectra, we plot the anti-Stokes part of the PLE spectra in Fig. 3 as a function of the normalized detuning $\Delta E/k_B T$ in Fig. 4. To avoid overlap, the spectra are shifted vertically, by the factors indicated in the figure. At all temperatures, we observe a strong decrease of the PL intensity with increasing detuning, until it reaches a plateau, where it remains roughly constant until the detuning exceeds an

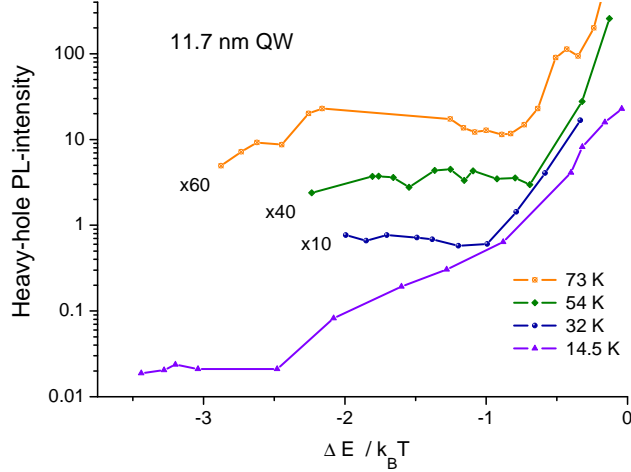


Figure 4. Integrated and normalized intensity of anti-stokes PL as a function of $\Delta E/k_B T$ for the 11.7 nm QW at various temperatures. The data are displaced vertically to avoid overlap.

energy of about $2k_B T$, where the decrease continues. The height of the plateau, relative to the value for resonant excitation, is in all cases between 0.01 and 0.03.

3.2 Cooling rate

If we consider the behavior observed in the last section with respect to laser cooling, we can calculate the amount of energy that is removed by AS-PL as the product of the integrated PL intensity L_{AS} and the laser detuning ΔE :

$$Relative\ cooling\ rate = \int I_{PL}(E) \Delta E(E) dE \approx L_{AS} \Delta E.$$

The approximation holds for small linewidths, which is well fulfilled in our case, as evidenced by the PL spectra. The definition corresponds to the radiative recombination term in the model of Sheik-Bahae and Epstein.⁸ To achieve net cooling, the relative cooling rate must be maximized to compensate the parasitic heating effects. Fig. 5 shows the measured data corresponding to the above equation for the 11.7 nm QW at three different temperatures. We observe for all temperatures above 20 K an increase of the cooling rate with increasing laser detuning $|\Delta E|$, a maximum close to $\Delta E \approx -2k_B T$, and a decrease at larger (absolute) detunings.

3.3 Upconversion between heavy holes and light holes

The data presented in Fig. 3 indicate efficient conversion from light holes to heavy holes. While this conversion is a simple thermalization, which increases the sample temperature, it is also possible to observe the opposite process, i.e. the excitation of heavy hole excitons and the observation of light-hole PL, indicating thermally activated up-conversion of heavy-holes to light-holes. Fig. 6 shows the PLE spectrum of the 11.7 nm QW at a temperature of 54 K, obtained by measuring the PL at the light-hole resonance and varying the laser excitation energy from -15 meV to +5 meV from the light-hole resonance.

The experimental data clearly show a large anti-Stokes PL yield for a detuning of $\Delta E = -10.7$ eV, which corresponds to resonant excitation of the heavy-hole exciton. With these parameters, the anti-Stokes process is doubly resonant: the absorption resonantly excites heavy-hole excitons, while the emission corresponds to a decay of light-hole excitons. In this case, the thermal energy is consumed by the conversion of heavy-holes to light-holes, as indicated in the inset in Fig. 4. The high efficiency of this process is also evidenced by the fact

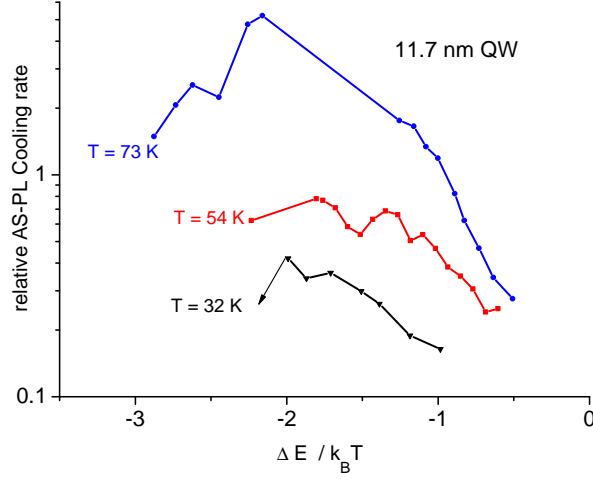


Figure 5. Relative cooling rate (integrated AS PL multiplied by the detuning $|\Delta E|$) as a function of $\Delta E/k_B T$ for 11.7 nm QW measured at 3 different temperatures.

that the anti-Stokes process with excitation of the heavy-hole yields more light-hole PL than resonant excitation at the light-hole transition.

In addition we should also mention that the lh energy of the 11.7 nm QW is higher than the hh energy of the 10.5 nm QW (see also fig 7 in sec. 4). The 10.5 nm QW is located closest to the surface in our sample. Therefore a part of its lh-PL is absorbed in the 10.5 nm QW. This means that in the case of a single QW sample this upconversion should be even higher.

The hh to lh upconversion can be observed for all QWs provided that the difference between the two states (hh and lh) is smaller or equal to the thermal energy $2k_B T$.

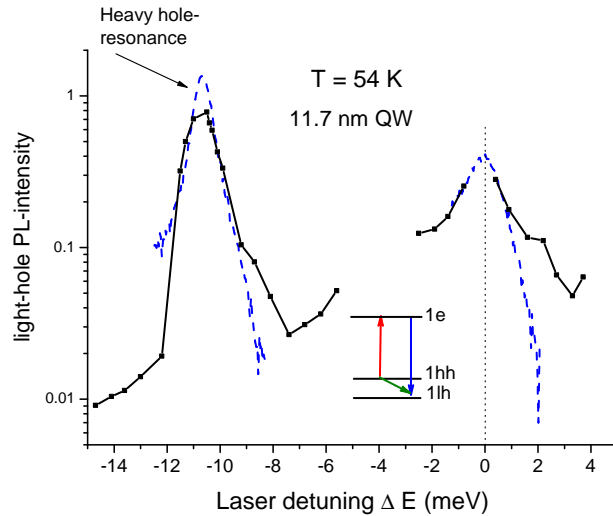


Figure 6. Normalized PL intensity of the light hole as a function of laser detuning ΔE at $T = 54$ K for the 11.7 nm QW. The peak at -10.7 meV corresponds to the heavy-hole resonance. The dashed blue lines indicate the corresponding PL-spectra at 54 K.

4. DEPENDENCE ON THE WELL WIDTH

In this section we compare the AS-PL for some of the QWs included in the sample at $T = 54$ K.

Fig. 7 shows the spectrum of the sample at this temperature. The excitation energy was 1.6376 eV. At this temperature, the amount of the thermal energy of the lattice ($2k_B T$) is high enough to allow us to measure the AS-PL over a wide detuning range, but the linewidth broadening of the individual QWs and therefore the overlap of their signals is not too large so that we can resolve and investigate the PL from the individual QWs with sufficient accuracy. As we can see in the Fig. 7, the higher energy levels of some thicker QWs are also excited. Together with the line width broadening at this temperature, this leads to an overlap of the PL lines in the region $E < 1.56$ eV. The PL energies and line widths (full width of half maximum, FWHM) of the various QWs at $T = 54$ K are listed in table 1.

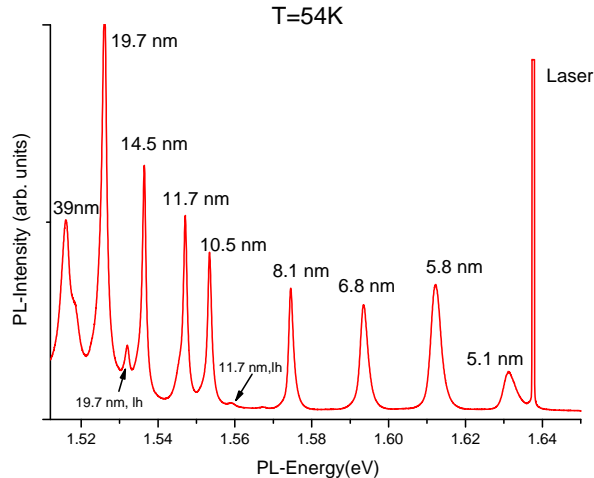


Figure 7. PL-Spectrum of the sample at $T = 54$ K. The excitation energy (laser) was 1.6377 eV.

Fig. 8 compares the results of the photoluminescence excitation (PLE) measurements for various QWs. The data points were obtained by integrating the PL-signal of the individual QWs (excluding the scattered laser light). The measured intensities are normalized to the intensity of the 19.7 nm QW. The intensity of the 19.7 nm QW is unnormalized, but vertically shifted for better comparison to the PL-intensity of the other QWs.

The width of the different PLE curves reflect the PL-FWHM of the corresponding QW. In the near resonance region, i.e. small $|\Delta E|$, the narrower the line width the steeper decreases the PL-intensity. This is due to smaller overlap between the PL and the laser line in the case of narrow linewidths. Outside this area in the anti-Stokes region $-2k_B T < \Delta E < -4meV$, the integrated PL-intensities of the most of QWs remain nearly constant and are comparable in the amplitude for the most of the QWs.

The shapes of PLE-curves for 14.5 nm and 8.1 nm QWs are slightly different from the shape of the other curves: in the region $-5.1 meV < \Delta E < -3.4 meV$, the PL of the 14.5 nm decreases because the laser energy becomes resonant to the lh-level of 19.7 nm QW. The same happens for the 8.1 nm QW, its intensity decreases in the region $\Delta E < -6.1 meV$, where the laser energy comes close to the lh-resonance of the 10.5 nm QW.

For the 10.5 nm QW, we could only measure the AS-PL up to $\Delta E = -5.1 meV$. After this point, the excitation energy comes into the resonance region of the 11.7 nm QW and due to the small energy distance of the two QWs, the PL of the 10.5 nm QW disappears completely under the PL-line of the 11.7 nm QW.

Our results indicate the importance of the Urbach tail in laser cooling of semiconductors as it was discussed by Khurgin.¹⁵ The thicker QWs are expected to be favored for AS emission due to their higher absorption cross

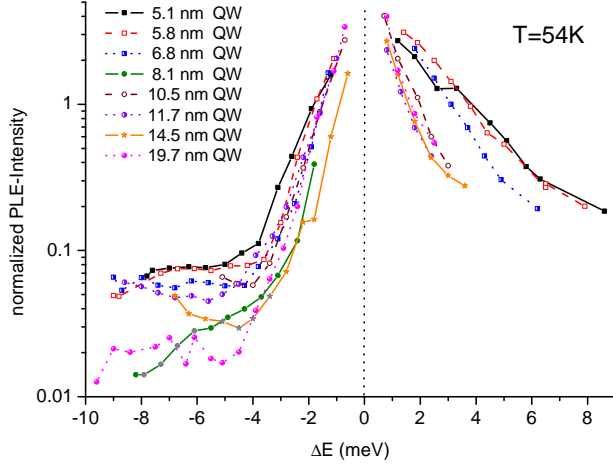


Figure 8. Photoluminescence excitation (PLE) measurements for QWs with various thicknesses. The temperature was kept constant at $T = 54$ K.

<i>QW thickness (nm)</i>	<i>PL-Energy (eV) T = 54 K</i>	<i>FWHM (meV) T = 54 K</i>
5.1	1.6312	3.7
5.8	1.6121	2.9
6.8	1.5933	2.2
8.1	1.5743	1.4
10.5	1.5533	1.2
11.7	1.547	1.2
14.5	1.5362	1.0
19.7	1.5259	1.3
39.3	1.5161	3.0

Table 1. PL-energy and full width of half maximum (FWHM) of various quantum wells at $T = 54$ K. The excitation energy was 1.6379 eV. The linewidth 39.3 nm QW is the FWHM of the main peak.

section. Their smaller linewidths, however, give rise, in the near resonant region, to a steeper decrease of their AS-PL-intensity with increasing detuning.

In the case of the 39.3 nm QW we can not provide a similar analysis of the AS-PL. The PL signal of this QW, as it is shown in fig. 9, consists of several peaks at about 1.516 eV, 1.518 eV and 1.522 eV corresponding to the ground and excited levels of the QW. The broader low energy peak at about 1.510 eV corresponds to exciton bound to carbon impurities. The inset of the figure shows the far resonance Stokes PL of the QW. The small energy difference between the energy levels and their overlap at this temperature complicates a quantitative analysis. Furthermore as we can see in the figure the anti-Stokes PL for this QW disappears rapidly with increasing ΔE (note the logarithmic scale) indicating that the PL-upconversion for this QW is less efficient than for the thinner ones.

The rapid decrease of the AS-PL for this QW is surprising: first the line width of this QW is relatively broad, in the same order as the line widths of the 5.1 nm and 5.8 nm QWs. Second the low energy tail of its PL is even more pronounced than the former QWs (see e.g. fig. 2 a). Furthermore the absorption cross section of this QW is larger than that of all other QWs. However a comparison of the PL spectra at 4.3 K (fig.1) and 54 K (fig.7) shows that the PL intensity of the 39.3 nm QW decreases relative to the other QWs more rapidly with

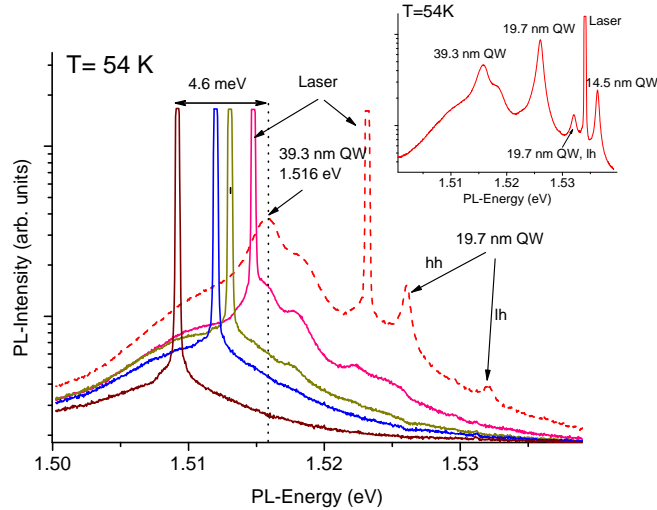


Figure 9. Stokes (dashed line) and anti-Stokes (solid lines) PL spectra of 39.3 nm QW at $T = 54$ K. The anti-stokes PL (logarithmic scale) disappears rapidly for this QW. The inset of the figure shows the far resonance Stokes PL of the QW.

increasing temperature.

As the exciton binding energy (\approx meV) increases with decreasing well width,²³ the strong AS-PL intensity of the thinner QWs indicates that the excitonic effects play a major role and should be taken into account to understand this behavior. However there are further investigation on broader QWs necessary to explain this behavior.

5. CONCLUSION

We presented a detailed experimental study of the anti-Stokes photoluminescence in GaAs QWs in a wide temperature range. The anti-Stokes PL intensity was measured as a function of laser detuning at various temperatures. Within a narrow region close to the exciton resonance, we observed a steep decrease of the PL intensity, which is almost symmetric for positive and negative detunings. For larger detunings the Stokes to anti-Stokes symmetry is broken and thermally activated processes become important. In this region the absorption cross section for the anti-Stokes PL is about 2-3 orders of magnitude lower than at the maximum of the resonance and increases with temperature. The highest relative cooling rates are obtained for laser detuning $\Delta E = E_{\text{laser}} - E_{\text{PL}}$ of about $2k_B T$.

We also measured the detuning dependence on the well width for various QWs consisting in the sample. The QWs with various thicknesses show a similar behavior in the large detuning ranges. Closed to the exciton resonance the intensity of the Anti-Stokes PL depends strongly on the linewidth of the individual QW. The narrower the linewidth the earlier the AS-PL decreases.

We were able to measure PL upconversion up to the room temperature even for QWs as thin as 3.9 nm, which shows that luminescence upconversion works at high temperatures efficiently even for narrow QWs, where the absorption cross section is relatively small. Furthermore we could measure a very efficient upconversion from heavy hole to light hole states in the case that the thermal energy, $2k_B T$, is in the same range as the energy difference between the levels.

In our study, we have only considered the absorption of the laser radiation, not taking into account loss mechanisms or parasitic absorption. Actual applications for laser cooling would have to account for these factors. Nevertheless our results show that it is possible to remove thermal energy from a semiconductor system by anti-stokes photoluminescence in all temperature ranges up to room temperature.

REFERENCES

- [1] Epstein, R. I., Buchwald, M. I., Edwards, B. C., Gosnell, T. R., and Mungan, C. E., “Observation of laser-induced fluorescent cooling of a solid,” *Nature* **377**, 500 (1995).
- [2] Hoyt, C. W., Hasselbeck, M. P., Sheik-Bahae, M., R. I. Epstein, R. I., Greenfield, S., Thiede, J., Distel, J., and Valencia, J., “Advances in laser cooling of thulium-doped glass,” *J. Opt. Soc. Am. B* **20**, 1066 (2003).
- [3] Thiede, J., Distel, J., Greenfield, S. R., and Epstein, R. I., “Cooling to 208 K by optical refrigeration,” *Appl. Phys. Lett.* **86**, 154107 (2005).
- [4] Seletskiy, D., Hasselbeck, M. P., Sheik-Bahae, M., and Epstein, R. I., “Laser cooling using cavity enhanced pump absorption,” *Proc. of SPIE* **6461**, 646104 (2007).
- [5] Patterson, W., Bigotta, S., Sheik-Bahae, M., Parisi, D., Tonelli, M., and Epstein, R., “Anti-stokes luminescence cooling of Tm^3 doped BaY_2F_8 ,” *OPTICS EXPRESS* **16**, 1704 (2008).
- [6] Sheik-Bahae, M. and Epstein, R. I., “Optical refrigeration,” *nature photonics* **1**, 693 (2007).
- [7] Rayner, A., Heckenberg, N., and Rubinsztein-Dunlop, H., “Condensed-phase optical refrigeration,” *Journal of the Optical Society of America B* **20**, 1037–1053 (2003).
- [8] Sheik-Bahae, M. and Epstein, R. I., “Can laser light cool semiconductors?,” *Phys. Rev. Lett.* **92**, 247403 (2004).
- [9] Apostolova, T., Huang, D., Alsing, P. M., and Cardimona, D. A., “Comparison of laser cooling of the lattice of wide-band-gap semiconductors using nonlinear or linear optical excitations,” *Phys. Rev. A* **71**, 013810 (2005).
- [10] Huang, D., Apostolova, T., Alsing, P. M., and Cardimona, D. A., “Spatially selective laser cooling of carriers in semiconductor quantum wells,” *Phys. Rev. B* **72**, 195308 (2005).
- [11] Huang, D., Apostolova, T., Alsing, P. M., and Cardimona, D. A., “Theoretical study of laser cooling of a semiconductor,” *Phys. Rev. B* **70**, 033203 (2004).
- [12] Li, J., “Laser cooling of semiconductor quantum wells: Theoretical framework and strategy for deep optical refrigeration by luminescence upconversion,” *Phys. Rev. B* **75**, 155315 (2007).
- [13] Rupper, G., Kwong, N., and Binder, R., “Large excitonic enhancement of optical refrigeration in semiconductors,” *Phys. Rev. Lett.* **97**, 117401 (2006).
- [14] Rupper, G., Kwong, N. H., and Binder, R., “Optical refrigeration of GaAs: Theoretical study,” *Phys. Rev. B* **76**, 245203–1 (2007).
- [15] Khurgin, J. B., “Role of bandtail states in laser cooling of semiconductors,” *Phys. Rev. B* **77**, 235206 (2008).
- [16] Finkeiß, E., Potemski, M., Wyder, P., Vinò, L., and Weimann, G., “Cooling of a semiconductor by luminescence up-conversion,” *Appl. Phys. Lett.* **75**, 1258 (1999).
- [17] Gauck, H., Gfroerer, T., Renn, M., Cornell, E., and Bertness, K., “External radiative quantum efficiency of 96 % from a GaAs/GaInP heterostructure,” *Appl. Phys. A* , 143 (1997).
- [18] Eshlaghi, S., Worthoff, W., Wieck, A., and Suter, D., “Luminescence upconversion in GaAs quantum wells,” *Phys. Rev. B* **77**, 245317 (2008).
- [19] Landolt-Börnstein, [*Zahlenwerte und Funktionen aus Naturwissenschaft und Technik: Band 16 Halbleiter*], Springer Verlag (1982).
- [20] Feldmann, J., Peter, G., Göbel, E. O., Dawson, P., Moore, K., Foxon, C., and Elliott, R. J., “Linewidth dependence of radiative exciton lifetimes in quantum wells,” *Phys. Rev. Lett.* **59**, 2337 (1987).
- [21] Eickhoff, M., Lenzman, B., Flinn, G., and Suter, D., “Coupling mechanisms for optically induced NMR in GaAs quantum wells,” *Phys. Rev. B* **65**, 125301 (2002).
- [22] Eshlaghi, S., *GaAs/Al_xGa_{1-x}As Quantentöpfe: MBE-Wachstum, Charakterisierung und laterale Modulation mittels fokussierter Ionenstrahlen*, PhD thesis, Universität Dortmund, Bochumer Univ. Verlag (2000).
- [23] Gerlach, B., Wüsthoff, J., Dzero, M. O., and Smondyrev, M. A., “Exciton binding energy in a quantum wells,” *Phys. Rev. B* **58**, 10568 (1998).